ESKİŞEHİR TEKNİK ÜNİVERSİTESİ BİLİM VE TEKNOLOJİ DERGİSİ
C- YAŞAM BİLİMLERİ VE BİYOTEKNOLOJİ

Eskişehir Technical University Journal of Science and Technology
C -Life Sciences and Biotechnology

Estuscience – Life, 2024, 13 [2] pp. 100-117, DOI: 10.18036/estubtdc.1386713

RESEARCH ARTICLE

THE EFFECTS OF DIFFERENT SONICATION METHODS ON ALPHA-SYNUCLEIN PRE-FORMED FIBRILS

Hilal AKYEL [1, 2 *], Elham BAHADOR ZIRH [3], Selim ZIRH [4], Banu Cahide TEL [1]

[1] Pharmacology Department, Faculty of Pharmacy, Hacettepe University, Ankara, Turkey
hilalakyel34@gmail.com - 0000-0003-2841-6668

[2] Pharmacology Department, Faculty of Pharmacy, Baskent University, Ankara, Turkey
elhambahador1969@gmail.com - 0000-0002-6921-2365

[3] Histology and Embryology Department, Faculty of Medicine, TOBB Economy and Technology University, Ankara, Turkey
dr.szirh@gmail.com - 0000-0002-7962-6078

[4] Histology and Embryology Department, Faculty of Medicine, Erzincan Binali Yıldırım University, Erzincan, Turkey
banutel@hacettepe.edu.tr - 0000-0001-5453-1294

Abstract

Alpha-synuclein (α-syn) aggregation is associated with neuronal death and the pathological hallmark of Parkinson's disease (PD). The α-syn preformed fibril model (α-syn-PFFs), reflects α-syn aggregation and is currently used in PD studies. To pass through the cell membrane, long fibrils should be fragmented by sonication. In our study, the effects of temperature, pulse modifications and/or device type on the sonication of α-syn-PFFs were investigated. Sonication was performed ultrasonic bath and in laminar-flow cabinet with probe sonicator. Dilutions were made from 5 µg/µl α-syn-PFFs stock in sterile-filtered dH2O to a final concentration and volume of 0.1 µg/µl and 200µl, respectively. Sonication was performed in an ultrasonic bath containing water at 10°C for 1 hour. All probe sonications were performed at 30% amplitude for 1 minute and 20 repetitions. The effect of temperature on sonication has been evaluated by performing sonication at room temperature (RT), in ice and in ice surrounded by dry ice. Also, the effects of pulse duration on sonication were evaluated using pulse durations of 1second(sec) on/1sec off, 3sec on/3sec off and 5sec on/5sec off. Furthermore, by waiting one minute between each sonication cycle, the heat released by the probe was prevented from affecting the fibrillar structure. The particle size was measured in triplicate by dynamic light scattering method. For transmission electron microscopy, formvar/carbon-coated grids were run through ddH2O-sonicated fibril-uranyl acetate solutions and kept dry until examined. Due to the variation in breakage of long α-syn fibrils, the effect of different parameters on sonication was investigated. In comparison of pulse durations, 5sec on/5sec off application produced shorter fibrils. Comparing the temperature interventions, lowering the temperature decreased the fibril size at 1sec on/1sec off settings but increased it at 3sec on/3sec off and 5sec on/5sec off. However, the shortest fibrils were obtained by sonication for 5sec on/5sec off at RT.

Keywords

Sonication,
Alpha-synuclein,
Pre-formed fibril,
Particle size,
Transmission electron microscopy

Time Scale of Article

Received: 09 Kasım 2023
Accepted: 29 April 2024
Online date: 30 July 2024

1. INTRODUCTION

Parkinson's Disease (PD) is a neurodegenerative disorder caused by a progressive loss of dopaminergic neurons in the substantia nigra pars compacta (SNpc). Over the age of 65, it affects 1-2% of the population [1]. In addition to the motor symptoms of PD, non-motor symptoms accompany the disease in both

*Corresponding Author: hilalakyel34@gmail.com

premotor and late stages [2]. The presence of alpha-synuclein (α-syn) aggregates in Lewy bodies and neurites, which are specific markers of the disease, indicates its importance in the pathogenesis of PD [3].

α-syn is a protein that contains 140 amino acids and is found in an alpha-helical structure. The protein is mainly located at the presynaptic terminals of neurons, where it plays a crucial role in maintaining synaptic vesicular homeostasis and synaptic transmission [4,5]. Physiologically, α-syn exists as an unfolded monomer, tetramer [6], and multimer bound to lipid membranes (Figure 1) [7]. In pathological conditions, posttranslational modifications such as ubiquitination, phosphorylation and misfolding result in the formation of insoluble α-syn aggregates in the beta-sheet conformation [8]. Upon accumulation, aggregates form in the soma, axons, and dendrites, forming Lewy bodies and Lewy neurites, respectively. Fibrillar α-syn is one of the main components of Lewy bodies/neurites [9].

The aggregation of a monomeric α-syn is a multi-step process that begins with a nucleation reaction in which monomeric α-syn is converted into oligomers of varying sizes (dimers, trimers, low molecular weight, high molecular weight). The oligomers are then converted into protofibrils, which in turn give rise to the insoluble fibrils (Figure 1) [10-12].

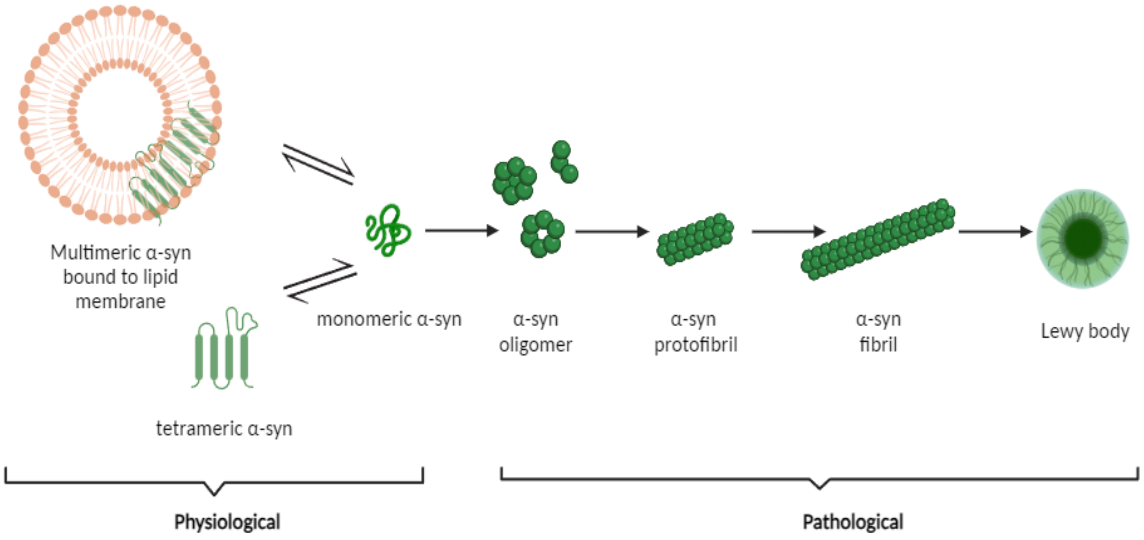

Figure 1. A process of forming α-syn fibrils. In physiological conditions, monomeric α-syn exists in equilibrium with multimeric structure bound to the lipid membrane and tetrameric structure. The formation of α-syn fibrils occurs in a nucleation reaction that transforms the soluble monomer into a beta-structured, stable, and insoluble fibril (designed with BioRender) [10].

The α-syn pre-formed fibril (α-syn-PFF) model is currently being used in PD research to recapitulate the Lewy pathology. In this model, exogenous α-syn fibrils trigger endogenous α-syn [13, 14] phosphorylating it at pS129, causing insoluble α-syn aggregates to form within the cell [15-21]. Therefore, the α-syn-PFF, which can mimic the pathogenesis of the disease in terms of α-syn aggregation and Lewy pathology, has gained increasing importance [22, 23].

In order for α-syn fibrils to be taken into the cell form the pathology *in vitro* or *in vivo*, fibrils should have a size between 50-100 nanometers (nm) or shorter in length. Long fibrils are therefore broken into short fragments using a probe sonicator or ultrasonic bath sonicator, which generates energy with vibration and sound waves, respectively [24, 25]. After sonication, a heterogeneous mixture of monomers, oligomers, and short fibrils is obtained [26-28]. Validation of sonication parameters is required to produce reliable *in vitro* and/or *in vivo* fibril models [24, 25]. Thus, it is necessary to investigate multiple sonication parameters [24, 25, 29]. Accordingly, sonication studies have shown that pulse duration, temperature of the experimental environment, sonication repetitions, and sonication device type vary.

In our study, we compared the effects of pulse duration, temperature, and sonication device type on 20 repeated sonications of α-syn-PFFs produced in the same series. After sonication, samples were analyzed using transmission electron microscopy (TEM). In addition, the hydrodynamic diameter-particle size was determined by dynamic light scattering (DLS).

2. MATERIALS AND METHODS

2.1. MATERIALS

Table 1: Experimental materials and equipments.

Equipment/Material Name	**Company**	**Catalog Number**
Human alpha-synuclein preformed fibrils	Produced in Ryan Lab and purchased from this lab	
Steril conical centrifuge tubes, 15 ml	Greiner Bio-One, Cellstar®	
Steril microcentrifuge tube, 1.5 ml	Greiner Bio-One, Cellstar®	
Parafilm	Parafilm M	PM-996
Stopper	Made in our laboratory	
Uranyl acetate	Eletron Microscopy Sciences	22400
Sterile-filtered deionized and distilled water		
Lockable tweezer		
Formvar/Carbon coated electron microscopy copper grids	Ted Pella Inc.	1801
Electron Microscopy Grids Box	Ted Pella Inc.	
Quartz cuvette		
Centrifuge Device	Hitachi	Himac CT6E
Probe sonicator	Sonics Vibra-Cell™	VCX 750
Probe	Sonics Vibra-Cell™ (microtip)	630–0422
Utrasonic bath sonicator	Branson	CPX5800H
Transmission electron microscope	FEI Tecnai™ G2 Spirit BioTwin model	
Device of Dynamic Light Scattering	Malvern Instruments, UK	Zetasizer Nano-ZS

2.2. METHODS

2.2.1. Sonication of α-syn-PFFs

Human α-syn fibrils was produced in Assoc Prof. Scott Ryan's laboratory (Ryan Lab, University of Guelph, Canada) as described [30] and purchased from this laboratory at a concentration of 5 µg/µl in a volume of 200 µl. α-syn fibrils were aliquoted until sonication and stored at -80°C in a volume of 4 µl. Sonication was carried out using a probe sonicator (Sonics Vibra-Cell™, VCX 750) and an ultrasonic bath sonicator (Branson-CPX5800H). After the α-syn fibrils were dissolved at room temperature, they were diluted with sterile-filtered deionized water to a final concentration of 0.1 µg/ml and a volume of 200 µl. Sterile centrifuge tubes (15 ml) were used for probe sonication and sterile microcentrifuge tubes for ultrasonic bath sonication.

2.2.1.1. Probe Sonication

Sonication was carried out in a laminar flow cabinet to avoid exposure to fibrils that may become aerosolized during sonication and to maintain sterility. A probe with a diameter of 3 mm was placed on a stabilizer in a laminar flow cabinet (Figure 2. a1, a2, a3). The probe was sterilized with 70% ethanol. Then, it was cleaned with distilled water and wiped dry. For 15 minutes, it was sterilized with UV light. The sterile centrifuge tube containing the fibrils (15 ml) is placed in tube holder during sonication at

room temperature. During sonications in ice and in ice surrounded by dry ice, the centrifuge tube was fixed with a white foam holder with a hole in the middle to prevent it from slipping. In the centrifuge tube containing 200 µl of diluted fibrils, a stopper was placed with an opening in the middle through which the probe can pass without touching the stopper. Due to the probe size, centrifuge tubes had to be used, even though the amount of sonicated liquid was much less. Therefore, a stopper was used to reduce the loss of liquid adhering to the wall or evaporating. The stopper was wrapped with parafilm to collect the liquid splashed on its surface by centrifugation.

The probe tip was inserted into the tube through the gap in the middle of the stopper. Sonication was performed by placing the probe tip in the center of a 200 µl solution to prevent volume loss. In order to avoid energy loss, the probe should not contact the walls of the tube or the stopper.
Sonication parameters are as follows:

a. The amplitude was set at 30%.
b. The total time was set at 00:01:00.
c. The pulse duration was set as 1 second (sec) on/1 sec off, 3 sec on/3 sec off, and 5 sec on/5 sec off, as shown in Table 2.
d. As shown in Table 2, the ambient temperature was adjusted to room temperature, ice, and ice surrounded by dry ice for each on/off period.
e. As shown in Table 2, there are 20 repetitions of sonication. The interval between repetitions should be one minute.

Upon completion of the sonication, the probe was removed from the solution and the tube was briefly centrifuged for 1 sec at 2000 rpm to collect the splashing liquid on the walls of tube. The sonicated samples were then placed in a sterile 1.5 ml microcentrifuge tube for imaging with TEM. The hydrodynamic diameter/particle size of the sample was measured by the DLS method by dilution of 2 µl of the sample with sterile-filtered deionized water to a final volume of 1000 µl (dilution ratio: 1:500). After each experiment, all surface of the laminar flow cabinet and probe tip was cleaned first with 1% sodium dodecyl sulfate (SDS) and then with 70% ethanol. The device was then sterilized for 15 minutes using ultraviolet light.

2.2.1.2. Ultrasonic Bath Sonication

The bath tank was filled with distilled water to the level indicated on the tank. Temperature of the water was set at 10°C. The fibrils in the 1.5 ml sterile microcentrifuge tube are fixed on the water surface with the holder so that the entire 200 µl volume is submerged in water. Sonication is performed for 1 hour. For TEM imaging, all 1.5 ml of a sterile microcentrifuge tube are used. In order to measure hydrodynamic diameter/particle size with DLS, 2 µl of the sample is diluted with sterile-filtered deionized water to a final volume of 1000 µl (dilution ratio: 1:500) [31].

Table 2: Protocols for sonication by probe and ultrasonic bath for α-syn-PFFs, respectively.

Sonication Technique	**Sonication Features**		
Probe	**Cycles/Duration**	**Pulse (on/off)**	**Temparature**
	20	1 sec / 1 sec 3 sec / 3 sec 5 sec / 5 sec	Room temperature Ice Ice surrounded by dry ice
Ultrasonic Bath	1 hour		Water temperature, 10 °C

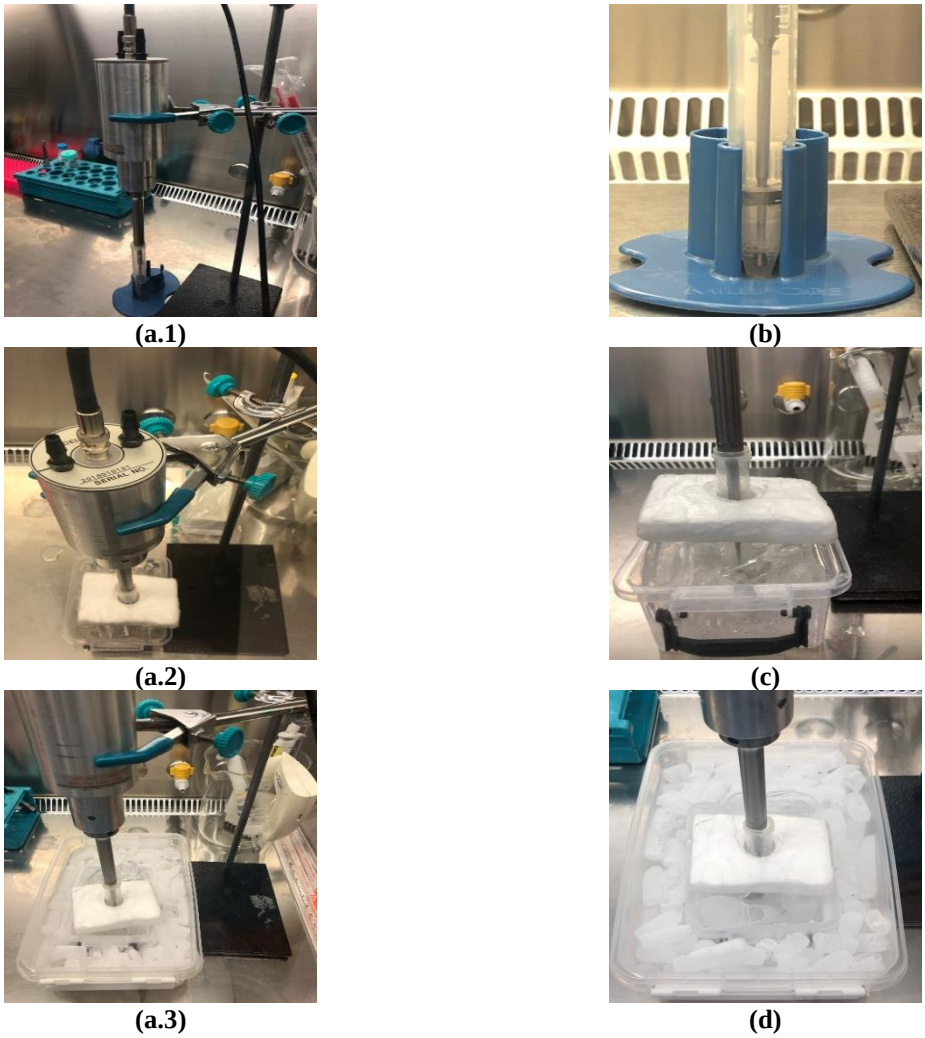

(a.1) **(b)** **(a.2)** **(c)** **(a.3)** **(d)**

Figure 2. Images of probe sonication. a.1, a.2, a.3. A view of the probe fixation from various angles. **b.** Sonication at room temperature. **c.** Sonication in ice. **d.** Sonication in ice surrounded by dry ice. **b, c, d.** For each protocol, a black stopper wrapped in parafilm prevents the aerosolized fibrils from evaporation. **c and d.** A white stabilizer prevents the 15 ml centrifuge tube from slipping.

2.2.2. Determination of Hydrodynamic Diameter/Size of Sonicated Fibrils

To measure the particle size in relation to the hydrodynamic diameter of the fibrils, dynamic light scattering (DLS) was performed at 25°C using a Malvern Instruments Zetasizer Nano-ZS (Malvern Instruments, Malvern, UK). After sonication, 1000 µl of sonicated fibrils in deionized water are transferred to a quartz cuvette for DLS measurements. For each sample, the measurement is repeated three times. As a result of the homogeneity of the sample, the device automatically determines the number of repetitions in measurement. A scattering angle of 90° is used for the measurement. The results of the measurement are displayed graphically in terms of the percentage density versus the hydrodynamic diameter (nanometer, nm) of the particles [29, 32].

2.2.3. TEM Imaging of Sonicated and Unsonicated Fibrils

The bench is covered with parafilm to prepare a clean-hydrophobic work surface then the sample, and the controls were dropped on where the grids would be immersed sequentially. 4 drops of 200 µL sterile-filtered distilled water (ddH_2O) dropped on parafilm. The entire volume of samples prepared for TEM was added as one drop; two drops of 200 µl 2% uranyl acetate were added. Formvar/carbon coated

copper grids were helded with fine tip lockable forceps. The dark side of the grid (formvar/carbon coating) was placed on the first drop of ddH2O. Once the grid has been removed after one minute, ddH2O is removed from the edge of the grid using a filter paper and the same procedure was repeated. Grids were placed on sonicated or unsonicated fibril drops for three minutes and excess fluids were removed with filter paper. After exposing the grids to the first drop of uranyl acetate for one-minute, excess uranyl acetate was removed with filter paper, and the process was repeated. Uranyl acetate process was carried out in the dark. Grids were kept in the third and fourth drops of ddH2O for one minute each, and the ddH2O was removed using filter paper on the grid edge (Figure 3). The grids were stored at room temperature in a grid box until imaging was performed [24]. The TEM imaging (FEI TecnaiTM G2 Spirit BioTwin model) was carried out by the TEM laboratory at Middle East Technical University, Central Laboratory. Fibrils and oligomers were imaged using magnifications of 13000 and 68000, respectively. The length of fibrils and diameter of oligomers, particles were measured three times using Image J 1.53k. Measurements were averaged from at least three scores.

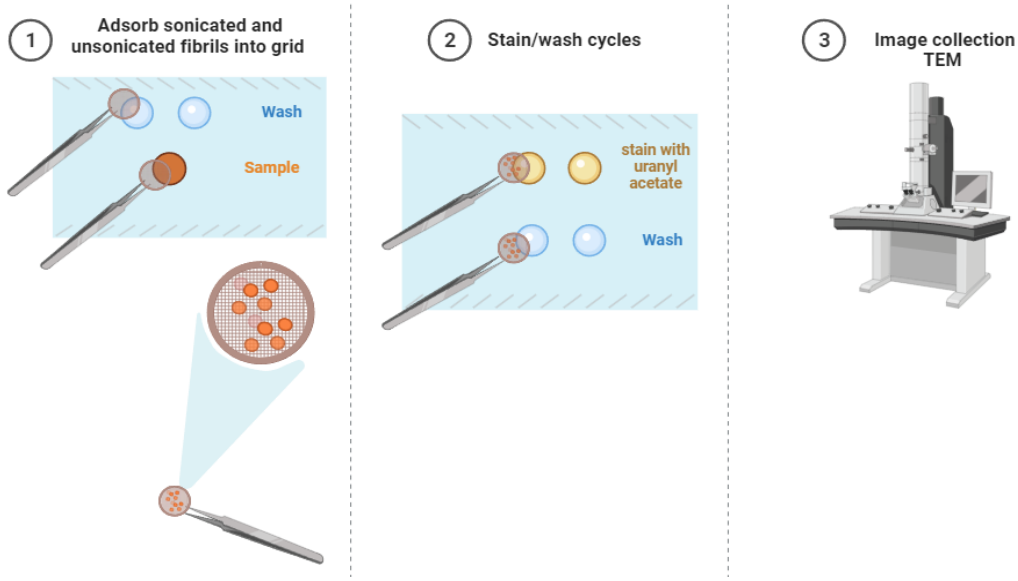

Figure 3. An illustration of the staining protocol for TEM. Grids were coated with formvar/carbon on their dark sides. 1) All drops were placed on parafilm. For one minute, the grid was floated in the first drop of ddH2O with the dark side touching the drop, and the excess was wiped off using filter paper. Application repeats for one minute with the second drop of ddH_2O, three minutes with one drop of sonicated or unsonicated fibrils, 2) for one minute with two drops of uranyl acetate, and for one minute with two drops of ddH2O. 3) Grids were stored in the grid box until they were displayed (designed with BioRender) [24].

2.2.4. Statistical Analysis

Results were presented as mean ± standard error. The Student's t test was used to compare two groups, and a one-way analysis of variance (ANOVA) followed by a *posthoc* Tukey's multiple comparison test was used to compare more than two groups. $p<0.05$ was considered statistically significant. The statistical analyses were conducted using GraphPad Prism 7 (GraphPad Software, Inc., San Diego, CA, USA).

3. RESULTS

3.1. Effects of Room Temperature on Sonication

The smallest particles were obtained with 5 sec on/off pulse by comparing other pulse durations with hydrodynamic diameters/particle sizes measured with DLS (Table 3). The size distribution of the

particles is shown in Figure 4. Since the measurement principle of the DLS device is optimized for spherical particles, the results obtained for fibrils and oligomers were considered as an indicator of the length alterations [33].

Table 3: Particle sizes obtained using probe sonication at room temperature (n = 3).

20 cycles and at room temperature			
Pulse (on/off)	1 sec on /1 sec off	3 sec on / 3 sec off	5 sec on / 5 sec off
Average Particle Size (diameter, nm)	2959 ± 1355	817,6 ± 75,61	290,4 ± 25,09

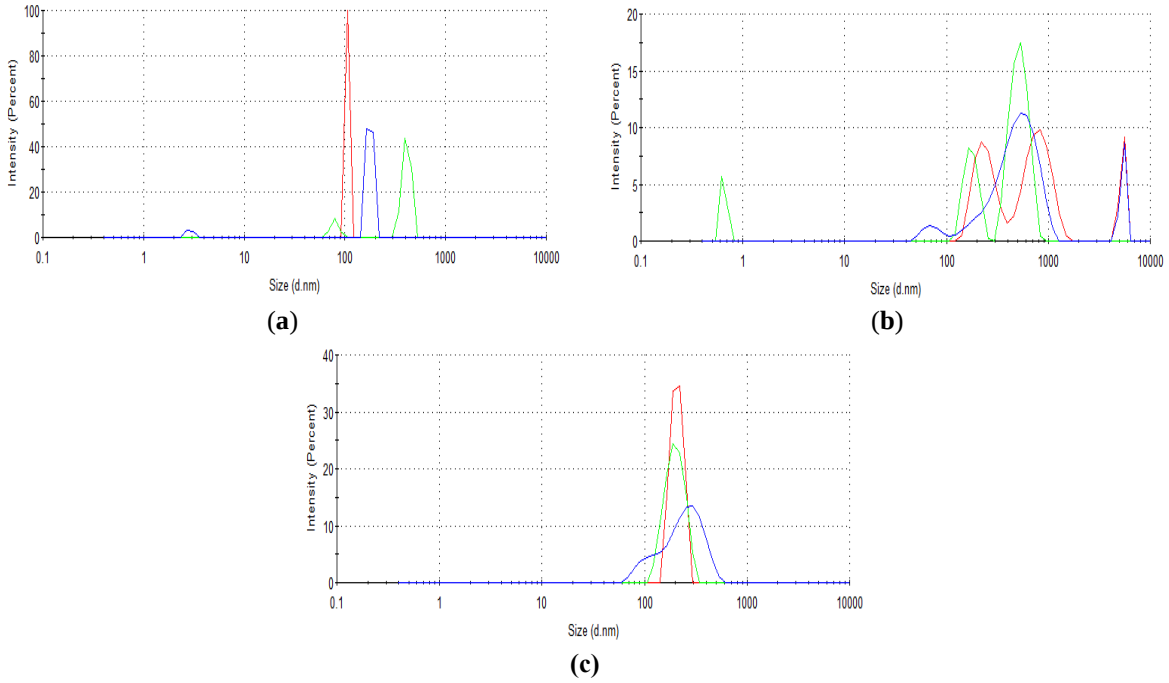

Figure 4. Particle size distribution obtained after sonication at room temperature. (**a)** 1 sec on/off, (**b)** 3 sec on/off, (**c)** 5 sec on/off (n = 3). The results of the measurement are displayed graphically in terms of the percentage density versus the hydrodynamic diameter (nm) of the particles.

As a result of TEM analysis, the average oligomer length (nm) was evaluated, and no significant differences were found in the 1 sec on/off or the 3 sec on/off group compared to the control. In the 5 sec on/off group, oligomer lengths were shorter on average than in the control or other pulse groups. ($p<0.0001$ 5 s on/off vs control, $p=0.0002$ 5 s on/off vs 1 s on/off, $p<0.0001$ 5 s on/off vs 3 s on/off, Figure 5.1). Although fibril length decreased in the pulse groups compared to the control group, significance was not reached (Figure 5.2).

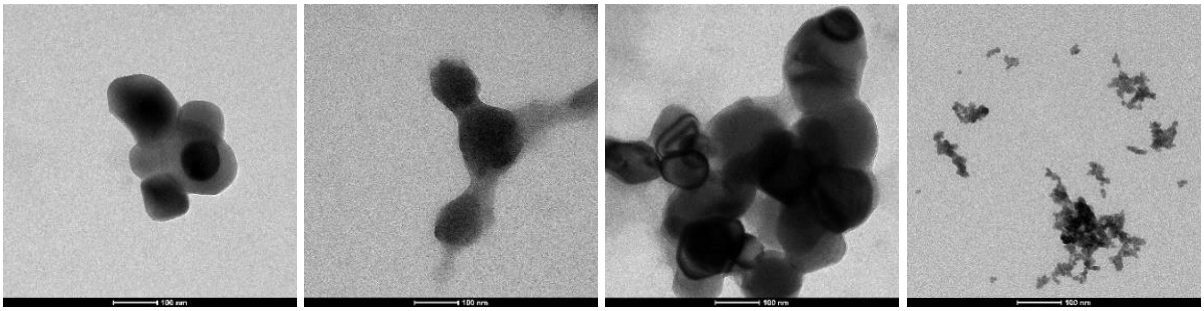

(a) **(b)** **(c)** **(d)**

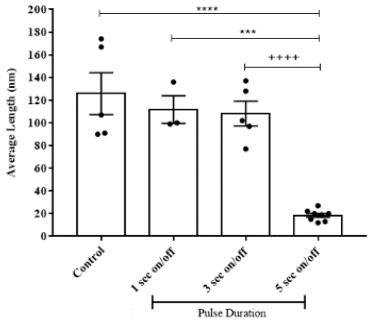

(e)

Figure 5.1. Oligomer lengths after probe sonication at room temperature. (**a)** Control, (**b)** 1 sec on/off, (**c)** 3 sec on/off, (**d)** 5 sec on/off. **e)** Data are expressed as mean ± standard error. One-way ANOVA followed by post hoc Tukey's multiple comparison tests were applied (****p<0.0001 5 s on/off vs control, ***p=0.0002 5 s on/off vs 1 s on/off, ++++p<0.0001 5 s on/off vs 3 s on/off). Scale bar: 100 nm.

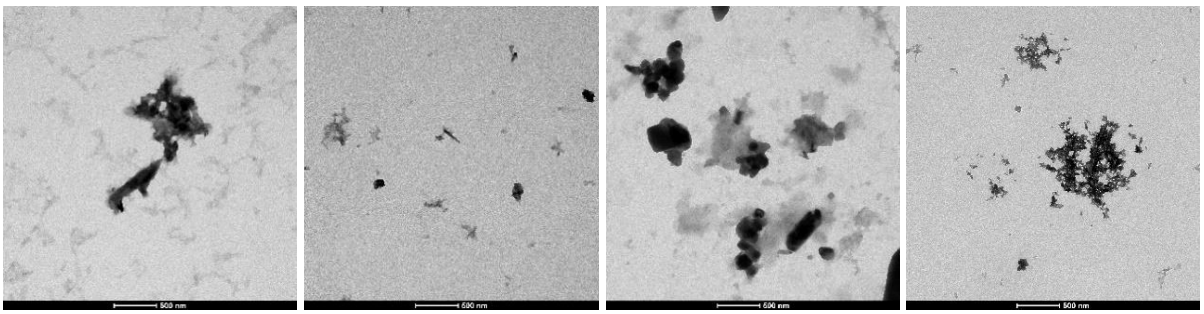

(a) **(b)** **(c)** **(d)**

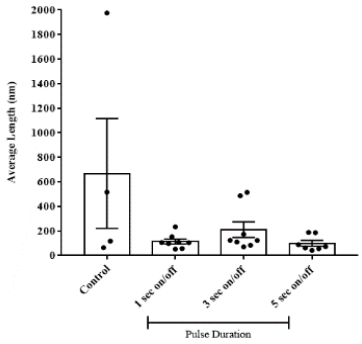

(e)

Figure 5.2. Fibril lengths after probe sonication at room temperature. (**a)** Control, (**b)** 1 sec on/off, (**c)** 3 sec on/off, (**d)** 5 sec on/off. (**e)** Data are expressed as mean ± standard error. One-way ANOVA followed by post hoc Tukey's multiple comparison tests were applied. Scale bar: 500 nm.

3.2. Effects of Ice on Sonication

Based on measurements of average hydrodynamic diameter/particle sizes with DLS, smaller particles were obtained in an ice compared to room temperature at 1 sec on/off and 3 sec on/off pulse durations. At the same time, the particles are smaller in size due to the longer pulse duration of 3 sec on/off as opposed to 1 sec on/off. In contrast, particle size increased at a 5 sec on/off pulse duration in ice as compared to room temperature (Table 4). The size distribution of the particles is shown in Figure 6. Since the measurement principle of the DLS device is optimized for spherical particles, the results obtained for fibrils and oligomers were considered as an indicator of the length alteration [33].

Table 4: Particle sizes obtained using probe sonication in ice (n = 3).

20 cycles and in ice			
Pulse (on/off)	1 sec on / 1 sec off	3 sec on / 3 sec off	5 sec on / 5 sec off
Average Particle Size (diameter, nm)	1443 ± 1108	494,1 ± 69,21	613,3 ± 105,9

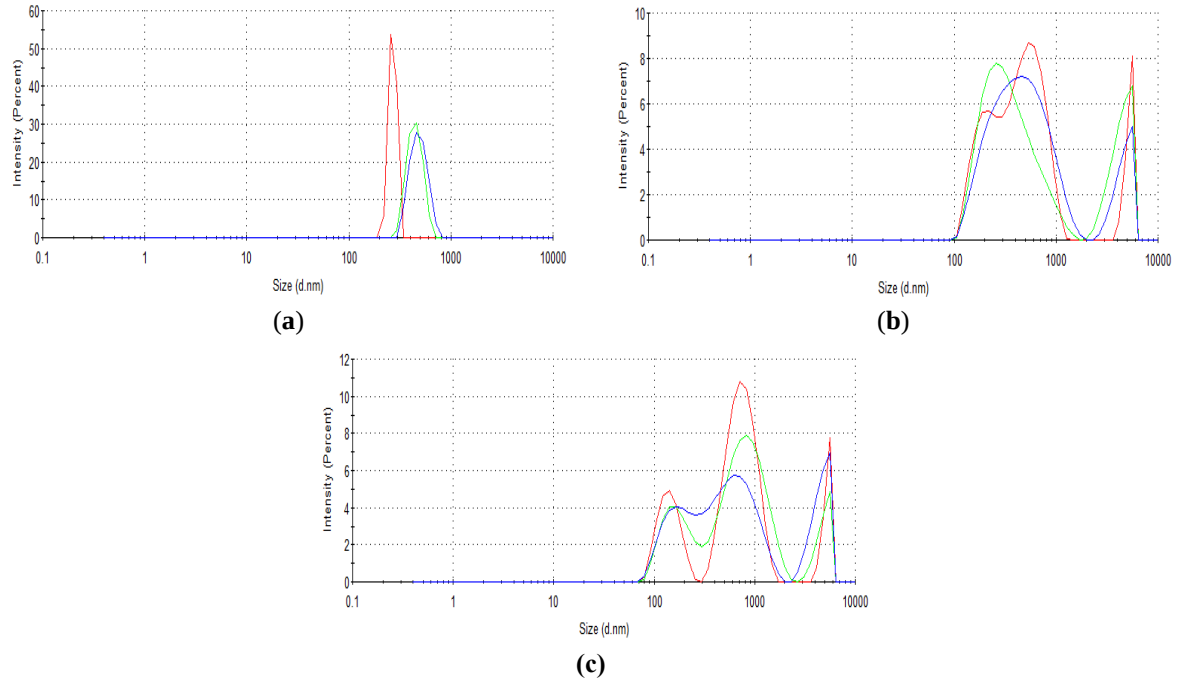

Figure 6. Particle size distribution obtained after sonication in ice. (**a)** 1 sec on/off, (**b)** 3 sec on/off, (**c)** 5 sec on/off (n = 3). The results of the measurement are displayed graphically in terms of the percentage density versus the hydrodynamic diameter (nm) of the particles.

Based on the TEM results, no difference was observed between the 1 sec on/off and the control, however, the average oligomer length of the 3 sec and 5 sec on/off groups was shorter than both the control and the 1 sec on/off group ($p=0.0001$ 3 s on/off vs control, $p=0.0002$ 3 s on/off vs 1 s on/off, $p<0.0001$ 5 s on/off vs control, $p<0.0001$ 5 s on /off vs 1 sec on/off, Figure 7.1). Although a decrease was observed in fibril length in the pulse groups compared to the control group, significance was not reached (Figure 7.2).

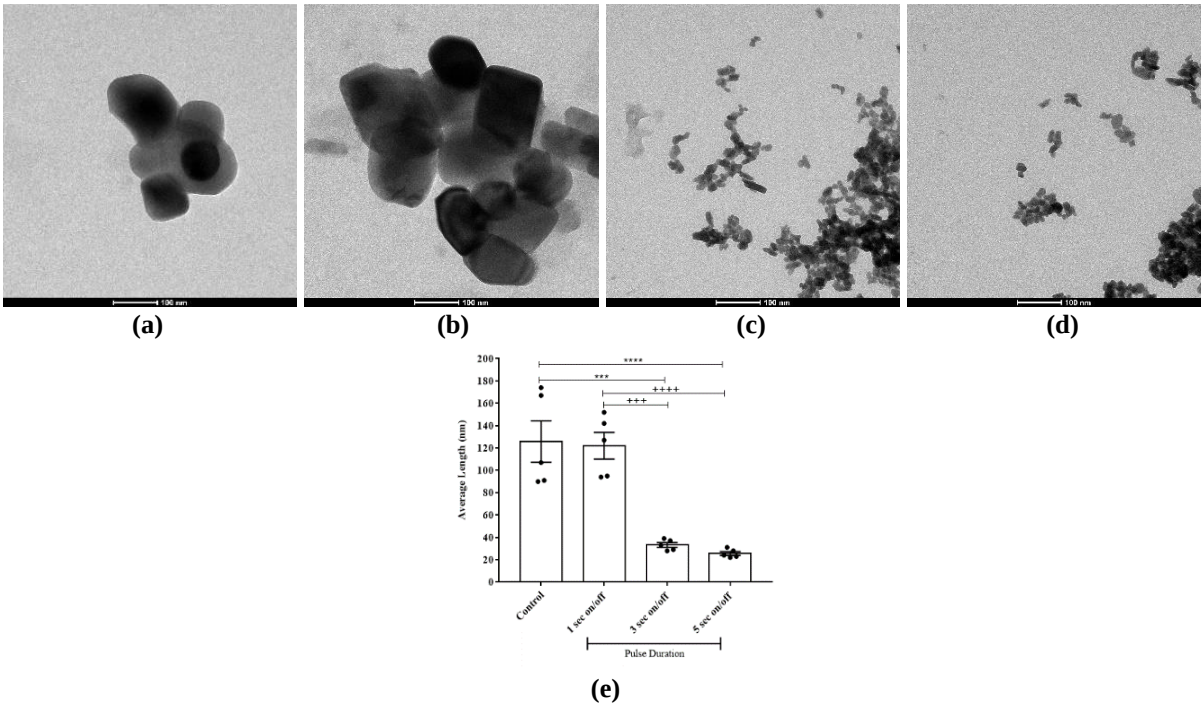

Figure 7.1. Oligomer lengths after probe sonication in ice. (**a)** Control, (**b)** 1 sec on/off, (**c)** 3 sec on/off, (**d)** 5 sec on/off. (**e)** Data are expressed as mean ± standard error. One-way ANOVA followed by post hoc Tukey's multiple comparison tests were applied (***p=0.0001 3 s on/off vs control, +++p=0.0002 3 s on/off vs 1 s on/off, ****p<0.0001 5 s on/off vs control, ++++p<0.0001 5 s on /off vs 1 sec on/off). Scale bar: 100 nm.

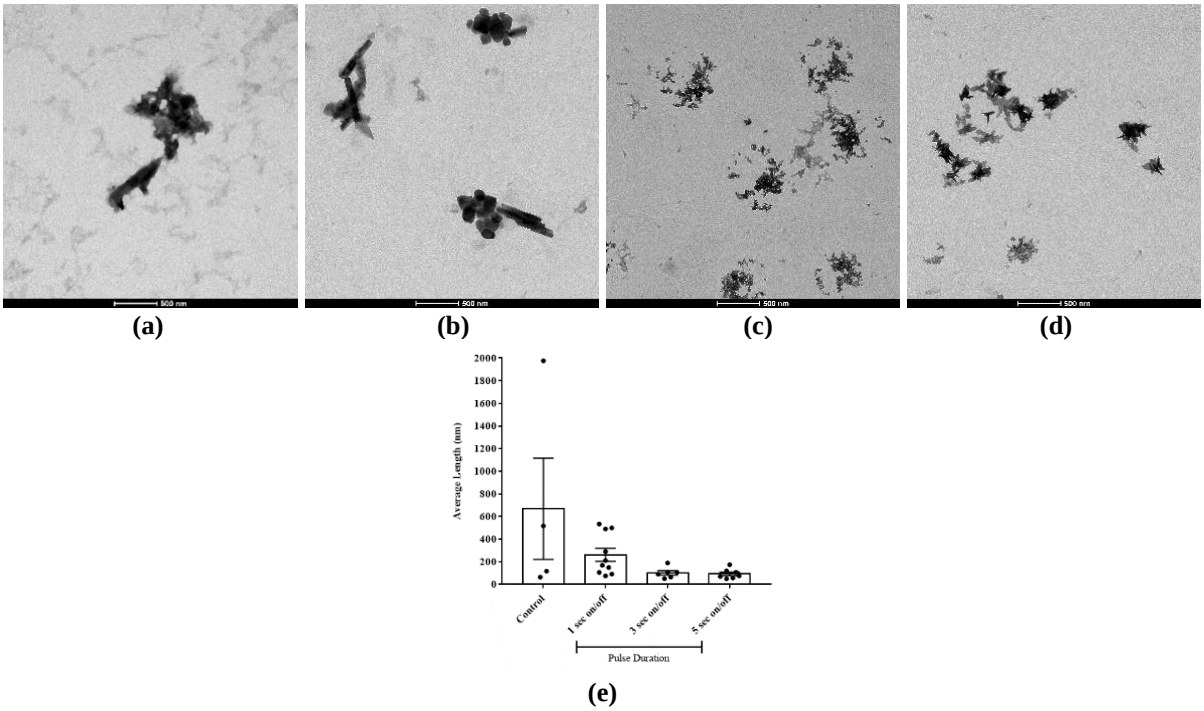

Figure 7.2. Fibril lengths after probe sonication in ice. (**a)** Control, (**b)** 1 sec on/off, (**c)** 3 sec on/off, (**d)** 5 sec on/off. (**e)** Data are expressed as mean ± standard error. One-way ANOVA followed by post hoc Tukey's multiple comparison tests were applied. Scale bar: 500 nm.

3.3. Effects of Ice Surrounded by Dry Ice on Sonication

Measurements of hydrodynamic diameter/particle size with DLS in ice surrounded by dry ice indicated smaller particles were obtained at a 1 sec on/off pulse than at other temperatures. In addition, 5 sec on/off pulse duration has the smallest particle size compared to other pulse durations. On the other hand, particle size increased at both 3 sec on/off and 5 sec on/off pulse durations as compared to other temperatures (Table 5). The size distribution of the particles is shown in Figure 8. Since the measurement principle of the DLS device is optimized for spherical particles, the results obtained for fibrils and oligomers were considered as an indicator of the length alteration [33].

Table 5: Particle sizes obtained using sonication in ice surrounded by dry ice (n = 3).

20 cycles and in ice surrounded by dry ice			
Pulse (on/off)	1 sec on / 1 sec off	3 sec on / 3 sec off	5 sec on / 5 sec off
Average Particle Size (diameter, nm)	1105 ± 786,8	840 ± 189,7	719 ± 262,4

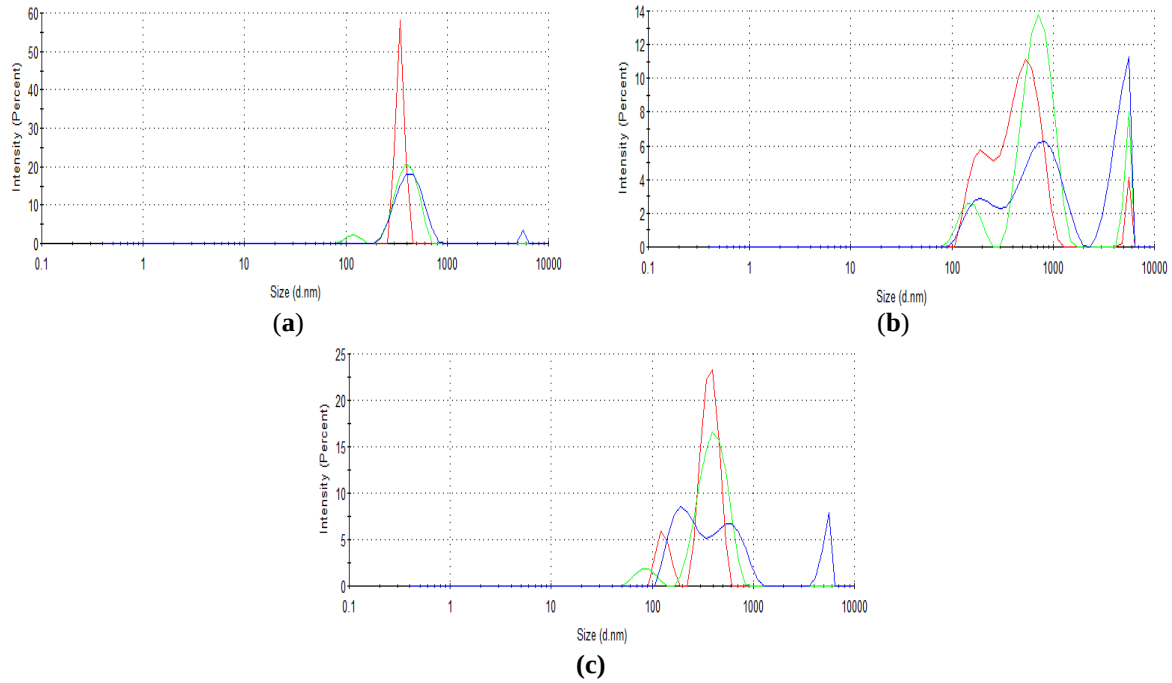

Figure 8. Particle size distribution obtained after sonication in ice surrounded by dry ice. (**a)** 1 sec on/off, (**b)** 3 sec on/off, (**c)** 5 sec on/off (n = 3). The results of the measurement are displayed graphically in terms of the percentage density versus the hydrodynamic diameter (nm) of the particles.

Based on the TEM results, there was no significant difference in the average oligomer length between the 3 sec on/off group and the control, but the average oligomer length was shorter in the 1 sec and 5 sec on/off groups than in the control (p=0.0011 1 sec on/off vs control, p=0.0007 5 sec on/off vs control). Furthermore, the average oligomer length was longer in the 3 sec on/off group than in the other pulse groups (p=0.0115 3 sec on/off vs 1 sec on/off, p=0.0091 3 sec on/off vs 5 sec on/off, Figure 9.1). Although fibril length was smaller in the pulse groups compared to the control, the difference was not statistically significant (Figure 9.2).

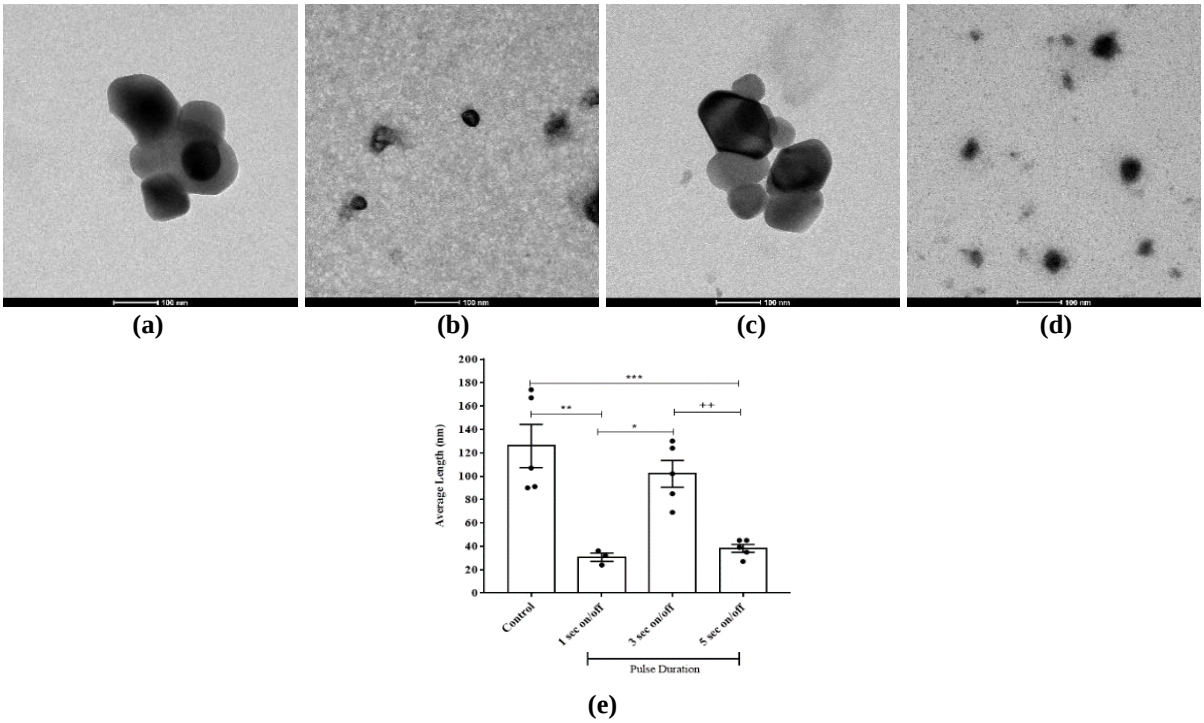

Figure 9.1. Oligomer lengths after probe sonication in ice surrounded by dry ice. (**a)** Control, (**b)** 1 sec on/off, (**c)** 3 sec on/off, (**d)** 5 sec on/off. (**e)** Data are expressed as mean ± standard error. One-way ANOVA followed by post hoc Tukey's multiple comparison tests were applied (**p=0.0011 1 sec on/off vs control, ***p=0.0007 5 sec on/off vs control, *p=0.0115 3 sec on/off vs 1 sec on/off, ++p=0.0091 3 sec on/off vs 5 sec on/off). Scale bar: 100 nm.

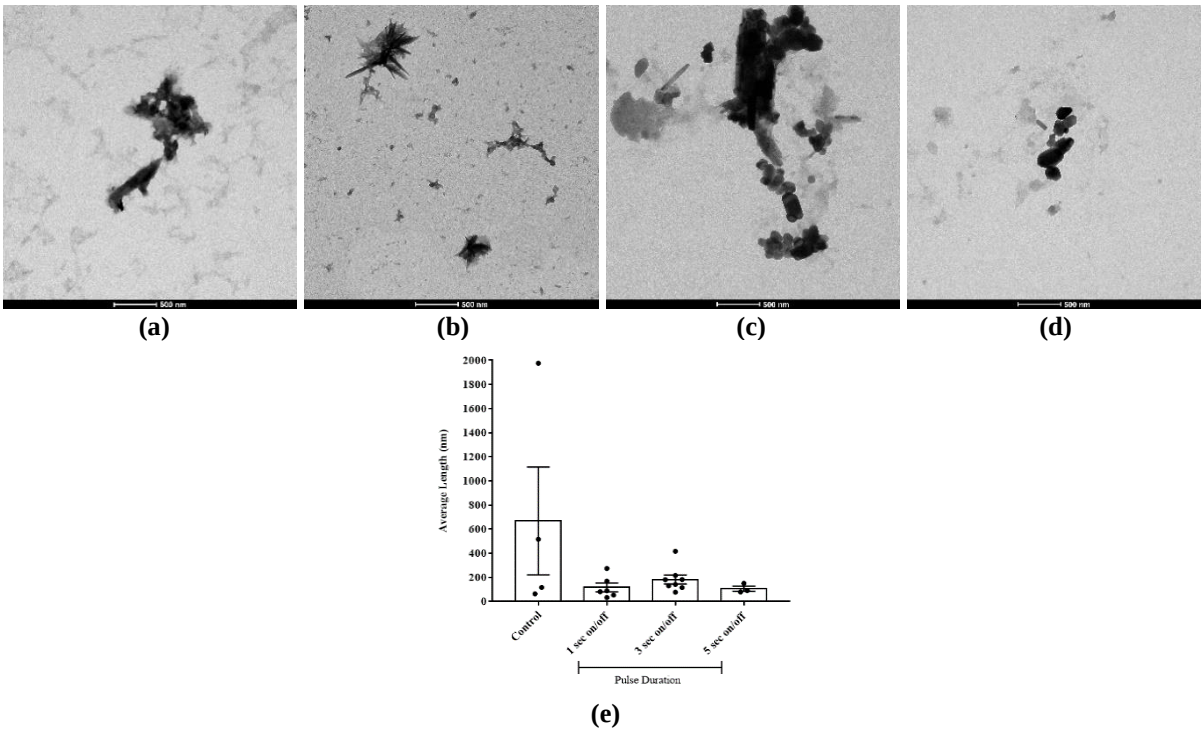

Figure 9.2. Fibril lengths after probe sonication in ice surrounded by dry ice. (**a)** Control, (**b)** 1 sec on/off, (**c)** 3 sec on/off, (**d)** 5 sec on/off. (**e)** Data are expressed as mean ± standard error. One-way ANOVA followed by post hoc Tukey's multiple comparison tests were applied. Scale bar: 500 nm.

3.4. Effects of Ultrasonic Bath on Sonication

A DLS measurement of the average hydrodynamic diameter/particle size revealed that the particle sizes were similar to those obtained by probe sonication (Table 6). The size distribution of the particles is shown in Figure 10. Since the measurement principle of the DLS device is optimized for spherical particles, the results obtained for fibrils and oligomers were considered as an indicator of the length alteration [33].

Table 6: Particle sizes obtained using ultrasonic bath sonication (n = 3).

	1 hour and 10 °C water temperature
Average Particle Size (diameter,nm)	1017 ± 116,4

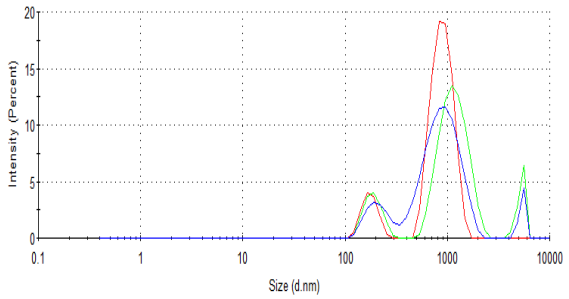

(a)

Figure 10. Particle size distribution obtained after ultrasonic bath sonication (n = 3). The results of the measurement are displayed graphically in terms of the percentage density versus the hydrodynamic diameter (nm) of the particles.

According to the TEM results, the oligomer lengths in the ultrasonic bath group were shorter than the control (p=0.0012 ultrasonic bath vs control, Figure 11.1). The length of fibrils was reduced in the ultrasonic bath group, but this difference was not statistically significant (Figure 11.2).

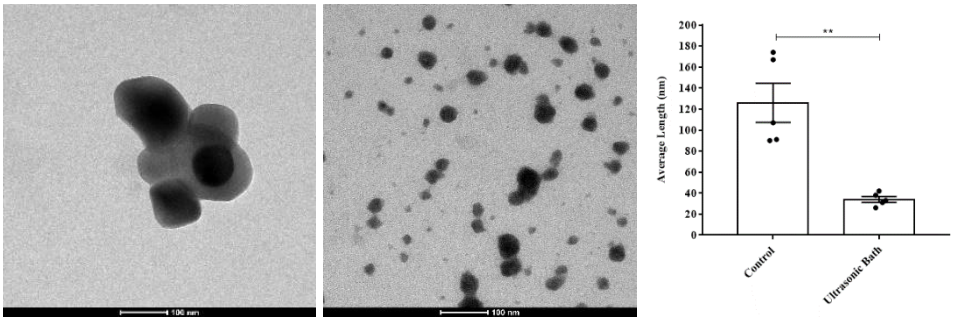

(a) **(b)** **(c)**

Figure 11.1. Oligomer lengths after ultrasonic bath sonication. (**a)** Control, (**b)** ultrasonic bath. (**c)** Data are expressed as mean ± standard error. Student's t test was applied (**p=0.0012 ultrasonic bath vs control). Scale bar: 100 nm.

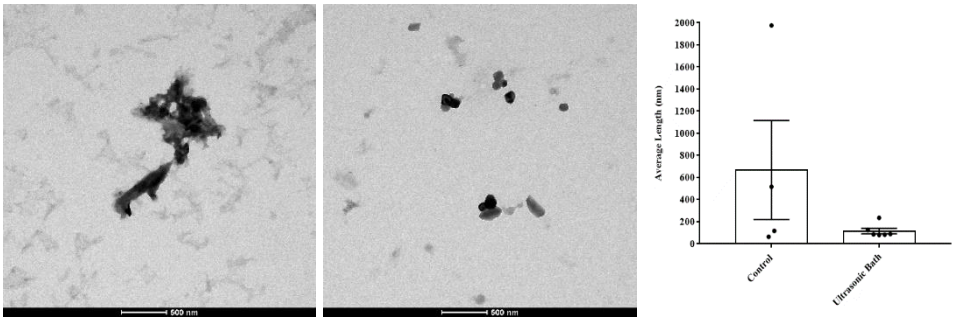

(a) **(b)** **(c)**

Figure 11.2. Fibril lengths after ultrasonic bath sonication. (**a)** Control, (**b)** ultrasonic bath. (**c)** Data are expressed as mean ± standard error. Student's t test was applied. Scale bar: 500 nm.

4. DISCUSSION

The α-syn-PFFs model provides the opportunity to elucidate the role of α-syn in PD pathogenesis and investigate therapeutic approaches. In order to investigate the pathology of α-syn, long fibrils were broken by sonication into short fibrils with an average length of 50-100 nm [26,28,34,35]. It has been demonstrated that the presence of fibrils ranging in length from 50-100 nm has a crucial role in the development of pathology following the uptake of α-syn into the cell [25, 36]. In fact, fibrils smaller than 50 nm resulted in more protein aggregation in both cultured cells and mouse brains [28].

Sonication protocols vary based on the type of sonicator (probe or bath sonicator), and the ambient temperature, pulse duration, and number of repetitions in probe sonication. Following sonication of fibrils, it is induced misfolding and aggregate formation of endogenous α-syn. However, ensuring the formation and reproducibility of α-syn pathology is a challenging process because of variations in the sonication protocol [26, 28]. Consequently, standard sonication protocols are required to break fibrils to the appropriate size and, hence, form pathology [24, 25].

Our study examined the effect of pulse durations at three different temperatures on fibrils breaking and found that shorter oligomers were obtained by increasing the pulse duration at room temperature after probe sonication. At room temperature, the oligomers were shorter than 50 nm when only a 5 sec on/5 sec off pulse was applied. The reduction in ambient temperature was found to decrease the oligomer size in pulse applications of 1 sec on/1 sec off (in ice surrounded by dry ice) and 3 sec on/3 sec off (in ice), whereas it increased the size in pulse application of 5 sec on/5 sec off. These results indicate that in order to break the fibrils, the ambient temperature should be reduced in accordance with the decreasing frequency of the pulse. Further, an increase in oligomer length was observed in ice surrounded by dry ice after a 3 sec on/3 sec off pulse, suggesting that monomers released during sonication may re-oligomerize even at sufficiently low temperatures [37]. At all temperature, however, the oligomers of 50 nm or shorter length were obtained by sonicating for a 5 sec on/5 sec off pulse. According to these results, fibrils were more effectively broken by consecutive pulse applications.

Besides probe sonication, ultrasonic bath sonication is also used as a sonication method [25,29,31]. In our study, the oligomers were 50 nm and shorter after ultrasonic bath sonication, consistent with prior study [31]. In ultrasonic bath sonication, fibrils do not aerosolize, thereby preventing fibril volume loss. In addition, the stopper used in our study reduced fibril volume loss during probe sonication. Using a stopper is an addition that contributes to the method in our study.

Although the fibril lengths were reduced following sonication with both the probe and ultrasonic bath, some fibrils were not broken. There may be a need to increase the number of sonication repetitions in order to break all fibrils, as has been observed in previous studies [28,38]. It is also recommended that

a waiting period was allowed between each sonication repetition during probe sonication in order to prevent the sample from overheating and to increase the success of the sonication process [39], as used in our study.

5. CONCLUSION

In conclusion, different sonication methods changed the sizes of the oligomers in our study. The results indicate that different sonication methods may be used to obtain oligomers of 50 nm and shorter lengths. It is also necessary to lower the ambient temperature in accordance with the decreasing pulse frequency. Additionally, there are some fibril structures that cannot be broken regardless of the method. Therefore, in future studies, the method should be improved by an increase in the number of sonication repetitions. In this way, identifying optimized/standard sonication protocols will contribute to the formation of α-syn pathology by using α-syn-PFFs model in PD studies.

ACKNOWLEDGEMENT

We would like to thank Assoc. Prof. Urartu Özgür Şafak ŞEKER, for providing the opportunity to work at Bilkent University, National Nanotechnology Research Center (UNAM), Şeker Lab, to carry out the sonication experiments, and PhD student Cemile Elif ÖZÇELİK for her help in the laboratory.

CONFLICT OF INTEREST

The authors stated that there are no conflicts of interest regarding the publication of this article.

CRediT AUTHOR STATEMENT

Hilal Akyel: Conceptualization, investigation, formal analysis, visualization, writing – original draft. **Elham Bahador Zırh:** Conceptualization, investigation, resources, visualization, writing – review & editing. **Selim Zırh:** Conceptualization, investigation, visualization, writing – review & editing. **Banu Cahide Tel:** Conceptualization, resources, writing – review & editing, supervision.

REFERENCES

[1] Poewe W, Seppi K, Tanner CM, Halliday GM, Brundin P, Volkmann J, Schrag AE, Lang, AE. Parkinson disease. Nat Rev Dis Primers 2017; 3: 1–21.

[2] Kalia LV, Lang AE. Parkinson's disease. The Lancet 2015; 386(9996): 896–912.

[3] Spillantini MG, Schmidt ML, Lee VMY, Trojanowski JQ, Jakes R, Goedert M. a-Synuclein in Lewy bodies. Nature 1997; 388: 839–840.

[4] Lashuel HA, Overk CR, Oueslati A, Masliah E. The many faces of α-synuclein: From structure and toxicity to therapeutic target. Nat Rev Neurosci 2013; 14(1): 38–48.

[5] Sulzer D, Edwards. RH. The Physiological Role of α-Synuclein and Its Relationship to Parkinson's Disease. J Neurochem 2019; 150(5): 475–486.

[6] Bartels T, Choi JG, Selkoe DJ. α-Synuclein occurs physiologically as a helically folded tetramer that resists aggregation. Nature 2011; 477(7362): 107–111.

[7] Burré J, Sharma M, Südhof TC. α-Synuclein assembles into higher-order multimers upon membrane binding to promote SNARE complex formation. PNAS 2014;, 111(40): 4274–4283.

[8] Rocha EM, De Miranda B, Sanders LH. Alpha-synuclein: Pathology, mitochondrial dysfunction and neuroinflammation in Parkinson's disease. Neurobiology of Disease 2018; 109: 249–257.

[9] Goedert M, Jakes R, Spillantini MG. The Synucleinopathies: Twenty Years on. J Parkinsons Dis 2017; 7: 53–71.

[10] Miraglia F, Ricci A, Rota L, Colla E. Subcellular localization of alpha-synuclein aggregates and their interaction with membranes. Neural Regen Res 2018; 13(7): 1136–1144.

[11] Tuttle MD, Comellas G, Nieuwkoop AJ, Covell DJ, Berthold DA, Kloepper KD, Courtney JM, Kim JK, Barclay AM, Kendall A, et al. Solid-state NMR structure of a pathogenic fibril of full-length human α-synuclein. Nat Struc Mol Biol 2016; 23(5): 405–417.

[12] Brás IC, Outeiro TF. Alpha-synuclein: Mechanisms of release and pathology progression in synucleinopathies. Cells 2021; 10(2): 1–19.

[13] Mao X, Ou MT, Karuppagounder SS, Kam TI, Yin X, Xiong Y, Ge P, Umanah GE, Brahmachari S, Shin JH, et al. Pathological α-synuclein transmission initiated by binding lymphocyte-activation gene 3. Science 2016; 353(6307).

[14] Masaracchia C, Hnida M, Gerhardt E, Lopes da Fonseca T, Villar-Pique A, Branco T, Stahlberg MA, Dean C, Fernández CO, Milosevic I, et al. Membrane binding, internalization, and sorting of alpha-synuclein in the cell. Acta Neuropathol Commun 2018; 6(1): 79.

[15] Luk KC, Song C, O'Brien P, Stieber A, Branch JR, Brunden KR, Trojanowski JQ, Lee VMY. Exogenous α-synuclein fibrils seed the formation of Lewy body-like intracellular inclusions in cultured cells. PNAS 2009; 106(47): 20051–20056.

[16] Luk KC, Kehm VM, Zhang B, O'Brien P, Trojanowski JQ, Lee VMY. Intracerebral inoculation of pathological α-synuclein initiates a rapidly progressive neurodegenerative α-synucleinopathy in mice. J Exp Med 2012; 209(5): 975–988.

[17] Volpicelli-Daley LA, Luk KC, Patel TP, Tanik SA, Dawn M, Stieber A, Meany DF, Trojanowski JQ, Lee VM. Exogenous α-Synuclein fibrils induce Lewy body pathology leading to synaptic dysfunction and neuron death. Neuron 2011; 72(1): 57–71.

[18] Volpicelli-Daley LA, Luk KC, Lee VMY. Addition of exogenous α-synuclein preformed fibrils to primary neuronal cultures to seed recruitment of endogenous α-synuclein to Lewy body and Lewy neurite-like aggregates. Nat Protoc 2014; 9(9): 2135–2146.

[19] Thakur P, Breger LS, Lundblad M, Wan OW, Mattsson B, Luk KC, Lee VMY, Trojanowski JQ, Björklund A. Modeling Parkinson's disease pathology by combination of fibril seeds and α-synuclein overexpression in the rat brain. PNAS 2017; 114(39): 8284–8293.

[20] Gegg ME, Verona G, Schapira AHV. Glucocerebrosidase deficiency promotes release of α-synuclein fibrils from cultured neurons. Hum Mol Genet 2020; 29(10): 1716–1728.

[21] Ueda J, Uemura N, Sawamura M, Taguchi T, Ikuno M, Kaji S, Taruno Y, Matsuzawa S, Yamakado H, Takahashi R. Perampanel Inhibits α-Synuclein Transmission in Parkinson's Disease Models. Mov Disord 2021; *36*(7): 1554–1564.

[22] Carta AR, Boi L, Pisanu A, Palmas MF, Carboni E, De Simone A. Advances in modelling alpha-synuclein-induced Parkinson's diseases in rodents: Virus-based models versus inoculation of exogenous preformed toxic species. J Neurosci Methods 2020; 338: 108685.

[23] Karpowicz RJ, Trojanowski JQ, Lee VMY. Transmission of α-synuclein seeds in neurodegenerative disease: recent developments. Lab Invest 2019; 99(7): 971–981.

[24] Patterson JR, Polinski NK, Duffy MF, Kemp CJ, Luk KC, Volpicelli-Daley LA, Kanaan NM, Sortwell CE. Generation of alpha-synuclein preformed fibrils from monomers and use in vivo. J Vis Exp 2019; 2(148): 1–10.

[25] Polinski NK, Volpicelli-Daley LA, Sortwell CE, Luk KC, Cremades N, Gottler LM, Froula J, Duffy MF, Lee VMY, Martinez TN, et al. Best practices for generating and using alpha-synuclein pre-formed fibrils to model Parkinson's disease in rodents. J Parkinsons Dis 2018; 8(2): 303–322.

[26] Kumar ST, Donzelli S, Chiki A, Syed MMK, Lashuel HA. A simple, versatile and robust centrifugation-based filtration protocol for the isolation and quantification of α-synuclein monomers, oligomers and fibrils: Towards improving experimental reproducibility in α-synuclein research. J Neurochem 2020; 153(1): 103–119.

[27] Pieri L, Chafey P, Le Gall M, Clary G, Melki R, Redeker V. Cellular response of human neuroblastoma cells to α-synuclein fibrils, the main constituent of Lewy bodies. Biochim Biophys Acta 2016; 1860(1): 8–19.

[28] Tarutani A, Suzuki G, Shimozawa A, Nonaka T, Akiyama H, Hisanaga SI, Hasegawa M. The effect of fragmented pathogenic α-synuclein seeds on prion-like propagation. J Biol Chem 2016; 291(36): 18675–18688.

[29] Singh V, Castellana-Cruz M, Cremades N, Volpicelli-Daley, LA. Generation and sonication of α-synuclein fibrils. Protocols.io 2020; 1–13.

[30] Ryan T, Bamm V V, Stykel MG, Coackley CL, Humphries KM, Jamieson-Williams R, Ambasudhan R, Mosser DD, Lipton SA, Harauz G, et al. Cardiolipin exposure on the outer mitochondrial membrane modulates α-synuclein. Nature Communications 2018; 9(1): 1–17.

[31] Creed RB, Memon AA, Komaragiri SP, Barodia SK, Goldberg MS. Analysis of hemisphere-dependent effects of unilateral intrastriatal injection of α-synuclein pre-formed fibrils on mitochondrial protein levels, dynamics, and function. Acta Neuropathol Commun 2022; 10(1): 1–19.

[32] Afitska K, Fucikova A, Shvadchak VV, Yushchenko DA. α-Synuclein aggregation at low concentrations. Biochim Biophys Acta Proteins Proteom 2019; 1867(7–8): 701–709.

[33] Kaplan M, Öztürk K, Öztürk SC, Tavukçuoğlu E, Esendağlı G, Calis S. Effects of particle geometry for PLGA-based nanoparticles: prepation and in vitro/in vivo evaluation. Pharmaceutics 2023; 15(1): 175.

[34] Mahul-Mellier AL, Vercruysse F, Maco B, Ait-Bouziad N, De Roo M, Muller D, Lashuel HA. Fibril growth and seeding capacity play key roles in α-synuclein-mediated apoptotic cell death. Cell Death and Differentiation 2015; 22(12): 2107–2122.

[35] Mahul-Mellier AL, Burtscher J, Maharjan N, Weerens L, Croisier M, Kuttler F, Leleu M, Knott

GW, Lashuel HA. The process of Lewy body formation, rather than simply α-synuclein fibrillization, is one of the major drivers of neurodegeneration. PNAS 2020; 117(9): 4971–4982.

[36] Xue WF, Hellewell AL, Gosal WS, Homans SW, Hewitt EW, Radford SE. Fibril fragmentation enhances amyloid cytotoxicity. J Biol Chem 2009; 284(49): 34272–34282.

[37] Shvadchak VV, Claessens MMAE, Subramaniam V. Fibril breaking accelerates α-synuclein fibrillization. J. Phys. Chem. B 2015; 119(5): 1912–1918.

[38] Redmann M, Wani WY, Volpicelli-Daley L, Darley-Usmar V, Zhang J. Trehalose does not improve neuronal survival on exposure to alpha-synuclein pre-formed fibrils. Redox Biology 2017; 11: 429–437.

[39] Abdelmotilib H, Maltbie T, Delic V, Liu Z, Hu X, Fraser KB, Moehle MS, Stoyka L, Anabtawi N, Krendelchtchikova V, Volpicelli-Daley LA, West A. Alpha-synuclein fibril-induced inclusion spread in rats and mice correlates with dopaminergic neurodegeneration. Neurobiol Dis 2017; 105: 84-98.